ELSEVIER

International Journal of Mass Spectrometry 208 (2001) 37–57

International Journal of Mass Spectrometry

Ag ion formation mechanisms in molten glass ion emitters

G.F. Kessinger, T. Huett, J.E. Delmore*

Idaho National Engineering and Environmental Laboratory, Idaho Falls, Idaho 83415-2208, USA

Received 7 November 2000; accepted 13 February 2001

Abstract

Experimental and computational studies were conducted on silver/molten borosilicate glass (silica gel) ion emitters to better understand the physical and chemical processes associated with them, and in particular the chemistry of the molten glass solution that enhances ion emission. Based on the results of these studies and previous work, a model is proposed that explains the major features of the observed phenomena. It is believed that the molten glass dissolves both the analyte element and some Re from the filament. Rhenium is oxidized by the B_2O_3 of the borosilicate glass producing a rhenium oxide that migrates to the surface of the glass, providing a high work function surface that enhances cation emission. Last, we believe the analyte element (in this case Ag) resides in the glass primarily in the zero oxidation state (reduced by thermal decomposition of the oxide or nitrate) and volatilizes from the surface with a percentage of Ag atoms volatilizing as cations determined by the difference between the work function of the surface and the ionization potential of the analyte atom. This explanation may be applicable to other elements analyzed by silica gel technology that are readily reduced to the elemental form (by thermal decomposition or by reduction by the Re filament). Selected features of this explanation, such as analyte solubility and a high work function surface, may be applicable to analyte elements that are not readily reduced to elemental form. (Int J Mass Spectrom 208 (2001) 37–57) © 2001 Elsevier Science B.V.

Keywords: Isotope ratios; Thermal ion emission; Silica gel; Molten glass; Ion emission mechanisms

1. Introduction

The thermal ion formation process generally termed the "silica gel" method has been widely used for isotope ratio measurements by thermal ionization mass spectrometry (TIMS) since its introduction in 1969 [1]. The original study concerned the analysis of lead (Pb), but also indicated that the method could produce ions from other elements. Subsequently, other investigators extended the method for the analysis of many other elements [1–19]. The original method involved dissolving the element to be analyzed in aqueous solution and adding it and phosphoric acid to hydrated silica gel, followed by drying and heating. This procedure results in the production of molten glass, although the presence of the glass phase was not mentioned by the developers or by many subsequent investigators. This molten solution, supported by a refractory metal filament, generally Re, constituted the emitter. Other investigators discovered that boric acid worked as well as, and in some cases better than, phosphoric acid to produce the emission-enhancing glasses [20–22]. The fundamental mechanisms by which these processes produce ions remain poorly understood, although in an earlier publication

* Corresponding author. E-mail: JED2@inel.gov

PII S1387-3806(01)00378-5

[23] a few of the features were identified. The present study was undertaken in an effort to gain a more complete understanding of the processes that govern these ion emission mechanisms. The main reason for modeling the borosilicate glass system, as opposed to a system based on silicate/phosphate glass, is that there is a more complete set of thermodynamic data at high temperatures for the B–O system than for the P–O system.

At the beginning of the present study it was speculated that ions might be pre-forming in the condensed phase and simply volatilized as ions, because in essentially all applications of this technique the analyte element was introduced into the mixture as an ion in an aqueous solution. This mixture is subsequently evaporated to dryness on the filament and the dried residue is melted into a glass in the instrument just prior to analysis. An argument against the existence of pre-formed ions is that most elements analyzed by this method produce the univalent atomic cation, which is analyzed by the mass spectrometer, whereas the majority of these elements do not exhibit a stable univalent cation in the condensed phase. This observation led to the choice of Ag to test this hypothesis of pre-formed ions because most commonly encountered Ag compounds only have zero and univalent oxidation states, and hence Ag could conceivably volatilize as a pre-formed univalent cation if it were stable in the molten glass matrix.

The current studies have not uncovered evidence supporting the "pre-formed ion" theory, and the notion of pre-formed ions appears to be improbable for analyte elements such as Ag that are readily reduced to the zero oxidation state at elevated temperatures. Based on evidence presented in this study, it appears that the analyte element is reduced to the zero oxidation state in the condensed phase and the atoms volatilize as a mixture of both neutral and ionic atomic species. Both the computational and the experimental work support the concept that the oxide based molten matrix is not able to maintain significant amounts of Ag above the zero oxidation state at operational temperatures.

The results of the present studies have led to two hypotheses. First, it is hypothesized that the ratio of ionic to neutral species volatilizing from the surface is determined largely by the work function of the surface and the ionization potential of the atom, and we present an explanation of how the molten glass solution can attain a work function large enough to result in the formation of ions of the abundance observed in the silica gel method. Second, it is hypothesized that the molten glass might successfully dissolve and "solvate" analyte atoms in the sample, resulting in individual atoms in the sample that would be free of significant complexation with other species or like atoms, allowing them to volatilize as atomic rather than as molecular species.

2. Experiment description

The bulk of the experimental work was performed on an ion/neutral mass spectrometer (I/N-MS) [24], which was used to make measurements of the masses and intensities of the thermal ions and the neutral species (by way of electron impact ionization) emitted from the samples. The identification of chemical processes occurring in the glasses was accomplished by recording mass spectra as a function of temperature, with these data being reduced to temperature profiles of various ions. Other experimental work was performed with a temperature programmed secondary ion mass spectrometer (TP-SIMS) that provided information on chemical species present on the surface at temperatures up to the maximum at which samples were analyzed.

2.1. Samples

The silver–borosilicate samples (AgBS) were synthesized from appropriate amounts of Ag metal (Johnson Matthey Electronics, powder 99.9% pure, 0.7–1.3 μm particles) or $AgNO_3$ (Aldrich 99.9999% pure), boric acid (Argent, reagent grade), and tetraethyl orthosilicate (Fischer, 98% pure). The constituents were mixed in an argon-filled glove box. After the mixture was removed from the glove box, approximately 10 mL of 0.05 M nitric acid was added to convert the tetraethyl orthosilicate to hydrated silica

gel. This method was chosen, as opposed to adding commercial silica gel, because hydrated silica gel has variable waters of hydration (and thus it is impossible to accurately measure the amount of SiO_2 present). The use of tetraethyl orthosilicate in a dry environment allowed the quantitative ratio of silicon to boron to be determined. Last, the amounts of $AgNO_3$ and silver metal added to the respective mixtures were such that the mole percentage of Ag in both materials would be the same. The silver–borosilicate samples were fabricated with nearly the same mole ratios of Ag, B, and silicon (1 mol Ag:1.71 mol Si:11.64 mol B) as the bismuth–borosilicate samples used in our earlier work with bismuth–borosilicate [23].

To prepare samples for analysis in the I/N-MS and the TP-SIMS, the silver–borosilicate mixtures described above or $AgNO_3$ or Ag_2O (Strem Chemicals, Inc. 99% pure) were mixed with de-ionized water and the solutions/slurries were transferred onto a flattened stainless steel tube that had been covered with Re (Goodfellow 99.99% pure, 0.05 mm thick) or Ta (Goodfellow 99.9% pure, 0.05 mm thick) sheet. The Re or Ta had been wrapped around the tube, and spot-welded to the stainless steel to secure it for the duration of the experiment. Care was taken so that the samples were not exposed to the stainless steel. Before the tube was flattened (done in an attempt ensure the temperature across the sample was uniform) a type K thermocouple was spot-welded to the inside of the tube. Re or Ta ribbons (used as resistive "heaters" to provide heat to the sample) were spot-welded onto the sides of the flattened stainless steel tube and onto sample mounting rods. The arrangement is shown schematically in Fig. 1. This emitter design was used because it essentially eliminates voltage drop across the sample face, which is known to cause defocusing in the ion lens around the ion emitting region [25], and because it provided a convenient mount for a thermocouple. The samples were slowly heated in air to evaporate the water, and the resulting condensed-phase material adhered to the Re or Ta filament.

The samples will be referred to using an abbreviated nomenclature. For example, the silver borosilicate (AgBS) made with $AgNO_3$ on Ta is referred to as AgBS/$AgNO_3$/Ta whereas the AgBS made with Ag on Re is referred to as AgBS/Ag/Re.

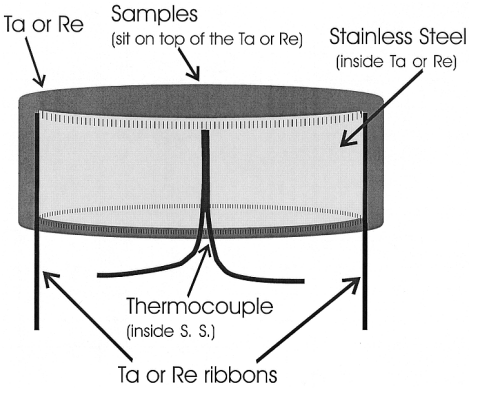

Fig. 1. Side cut away view of the sample mount. The thermocouple (black) was inside the flattened stainless steel tube (light gray). The Ta or Re ribbons (black) were spot-welded to the outside of the stainless steel tube but inside the Ta or Re. The Ta or Re (dark gray) was cut and spot-welded to the outside of the flattened tube so that no stainless steel was exposed. Samples were placed on top of the Ta or Re.

2.2. Ion/neutral mass spectrometry

The I/N-MS, which was designed in our laboratory [24], was built around an Extrel model no. 7-162-8 quadrupole mass spectrometer with 9.5 mm diameter rods and a model 041-11 electron impact (EI) ion source. The instrument could be switched between the neutral (EI) mode and the thermal ion (TIMS) mode by changing the computer controlled lens voltages and turning off the electron-emitting filament. Two sets of TIMS voltages were used, one for cations and the other for anions. The lens and sample filament voltages for all of the modes were determined through ion optics modeling with SIMION 6.0 [26] and verified experimentally. It was found that the voltages used for one mode effectively suppressed ion transmission from the other modes, even when the EI filament was emitting electrons. The ion source was modified so the sample filament protruded nearly 7 mm inside the first ion source cage. This modification not only increased the sensitivity of the instrument for neutral vapors and emitted ions but also allowed observation of evolved condensable vapors, such as

Ag, that otherwise could condense prior to reaching the ion formation region. The temperature was monitored with a Fluke 51 K/J digital thermocouple readout. During these experiments the rate of temperature increase was controlled manually by adjustment of the heating filament current; consequently, the rate of temperature increase was unique in each experiment. One aspect of the experimental procedure that would be performed differently were it to be repeated is that the temperature ramp would be much more closely controlled. A probable explanation for the spread in the width of some of the temperature profiles is that the heating rate was not closely controlled. A more closely controlled heating rate would have allowed a much better evaluation of the width of the profiles of gaseous species with temperature.

2.3. Temperature programmed secondary ion mass spectrometry

The TP-SIMS instrument was designed and built in our laboratory. It consists of an Extrel 2-2000 AMU quadrupole, a high-temperature probe that is inserted through a vacuum interlock, and a primary ion gun. The TP-SIMS experiments were performed with a ReO_4^- primary ion beam. The ReO_4^- was produced by heating a $Eu_2O_3/Ba(ReO_4)_2$ mixture which was processed into an ion source in our laboratory [27,28]. The ReO_4^- ions were accelerated to 10 keV and focused onto the sample so that a silhouette of the sample was observed on an image intensifier behind the sample. Based on visual observations, the primary ion beam impinged on the entire sample surface. The primary ion current varied from 70 to 100 pA, while the data acquisition times varied from 442 s for the samples on Ta to 492 s for the samples on Re. An arrangement similar to that used with the I/N-MS was used to measure the temperature during the TP-SIMS experiments.

The ions were extracted from the sample using pulsed extraction (alternately extracting secondary cations and anions), which was accomplished by continuously switching the polarity of the extraction field throughout the data collection; extraction gate times were tens of milliseconds. In this way the surface charge was minimized and both cations and anions were monitored [29]. Ions were detected both from TIMS and from secondary ion emission. Because the ion source focusing conditions for the surface ions and secondary ions are essentially identical (due to the fact that both types of ions originate from the surface of the sample) SIMS ions are identified from the difference (SIMS−TIMS) spectra. This was accomplished by subjecting the surface to the primary ion beam, measuring the ion beam intensity (both thermal and secondary ions), deflecting the primary beam and measuring the ion beam again (when only the thermal ions were produced), and then subtracting the thermal ion intensity from the combined intensity. The mass spectra were scanned from 10 to 450 u for the samples on Ta and from 10 to 500 u for the samples on Re.

The primary beam of perrhenate anions produced good quality SIMS spectra from these materials but its use precluded reliable observation of rhenium oxides in the SIMS spectra due to the possibility that implanted ions might be observed.

3. Experimental results

3.1. Features common to all samples

A feature common to all of the analyses was alkali metal ion emission from TIMS. All TIMS instruments have some background from alkali metal ions, which is thought to arise from filament materials and the glass insulators of the sample holder (the neutral species migrate up the posts to the hot filaments, where they volatilize as ions prior to reaching the molten glass). In addition, impurities in the molten glass may also contribute.

Another feature common to all analyses is the observation that the only Ag species ever detected from EI, TIMS, or SIMS are monatomic; no molecular ions were observed at any temperature in either the I/N-MS or the TP-SIMS. These observations are consistent with the hypothesis that Ag exists in the molten glass matrix as monatomic species, which is

consistent with the notion that Ag is dissolved and solvated in the molten matrix.

Another observation common to all measurements is that all Ag ions and neutrals were observed across a similar temperature range. Since a new thermocouple was required for each sample (placement was not always identical) and it was not possible to closely control the temperature ramps, there were some variations observed in the volatilization temperatures for the Ag species. Specifically, the initial observation of Ag^0 and Ag^+ were at similar temperatures, peaked at similar temperatures, and were exhausted at similar temperatures for all samples. For the samples that did not emit any thermal Ag^+ (all samples mounted on Ta and $AgNO_3$ without a glass matrix), Ag^0 volatilized across the same temperature range as for the other samples. These results support the argument that the production of Ag^0 and Ag^+ are from the same condensed phase species, which we believe to be elemental Ag. The fact that the molten glass matrix did not significantly raise the volatilization temperature of Ag over that observed for the samples that were not in the molten glass matrix suggests that there was not significant chemical interaction of Ag with the molten glass matrix.

3.2. Temperature programmed secondary ion mass spectrometry results

Temperature programmed SIMS experiments were performed to identify the secondary ions emitted from the filament materials (Re and Ta) in the temperature range (room temperature to approximately 1000 °C) of the ion–neutral experiments, from $AgNO_3$ or Ag_2O supported on the filament materials over the same temperature range, and from mixtures of $AgNO_3$ and borosilicate supported on the filament materials over the same temperature range. The primary purpose of these experiments was to characterize the behavior of Ag as the chemical environment changed in an attempt to elucidate the chemical behavior of the Ag present as the neat nitrate salt on the filament materials and in the borosilicate glass matrix on the filament materials.

In the experiments involving neat $AgNO_3$ salt on filaments, Ag^+ and NO_2^+ were the only species attributable to $AgNO_3$. During the experiments with Re filaments, the NO_2^+ signal was exhausted by the time the sample temperatures were raised to the 250–300 °C range. During the experiments with Ta filaments, NO_2^+ was still detectable at higher temperatures. This either indicates that nitrate reacts with Re at lower temperatures, or that it reacts at a faster rate than with Ta. No attempt was made to start these experiments with the same amount of nitrate salt or nitrate salt–borosilicate mixture, and we believe these temperature-dependent observations are probably strongly dependent on the amount of nitrate salt present.

No attempt was made to detect the temperatures at which the NO_2^+ signal disappeared during the studies of the $AgNO_3$-borosilicate mixture on Re; however, the only species attributable to the nitrate salt were Ag^+ and NO_2^+. The experiments involving the nitrate–borosilicate mixture supported on Ta presented a similar secondary ion spectra. Once again, we believe that the amount of material present influences the temperature at which the NO_2^+ disappears. As mentioned previously, the only Ag species observed was the Ag^+ ion, consistent with the concept that Ag is not extensively complexed in the molten glass matrix.

Last, the SIMS experiments involving the neat Re filament material showed no secondary ions containing Re over the entire temperature range and those with the neat Ta filament showed no Ta containing secondary ions.

3.3. Ion/neutral mass spectrometry results

3.3.1. Silver–borosilicate containing $AgNO_3$ on Ta

Species detected in the gas phase using EI (see Table 1) originate at the surface as neutral molecules. Normalized ion currents of these EI-generated ions versus filament temperature for AgBS/$AgNO_3$/Ta shown in Fig. 2 are trimodal. The first mode, at temperatures up to about 250 °C, is due to the desorption of water. Ions of $m/z = 16$ (O^+), 17 (OH^+), and 18 (H_2O^+) had the same temperature profile over the temperature range from 50 to about

Table 1
Ions detected from the four samples, using electron impact ionization of sublimed or evaporated neutrals and thermal ionization or emission of ions

Sample	Electron impact ionization: ions formed from neutrals	Thermal ionization or emission: cations from the surface	Thermal ionization or emission: anions from the surface
AgBS with $AgNO_3$ on Ta	O^+, OH^+, H_2O^+, NO^+, NO_2^+, Ag^+	Na^+, K^+	BO_2^-
AgBS with $AgNO_3$ on Re	O^+, OH^+, H_2O^+, NO^+, NO_2^+, Ag^+, Re^+, ReO^+, ReO_2^+, ReO_3^+, $HReO_3^+$, $HReO_4^+$, $Re_2O_7^+$ (weak)	Na^+, K^+, Ag^+	BO_2^-
AgBS with Ag on Ta	O^+, OH^+, H_2O^+, Ag^+	Na^+, K^+, Rb^+, Cs^+	BO_2^-
AgBS with Ag on Re	O^+, OH^+, H_2O^+, Ag^+	Na^+, K^+, Rb^+, Ag^+ Cs^+	BO_2^-

250 °C, and the relative ion abundances were consistent with the fragmentation pattern for water [30]. These ions are probably due to the desorption of water from the sample. The second mode, from about 250 to 650 °C, is due to the decomposition of the metal nitrate to form NO_2 which exhibits EI-generated ions at m/z = 16 (O^+), 30 (NO^+), and 46 (NO_2^+). These ions have the same temperature dependence for the temperature range 170–650 °C, have nearly constant ion abundance ratios and have the fragmentation pattern that is expected for NO_2 [30]. The third mode corresponds to the sublimation of Ag^0 at high temperatures. Signal due to Ag^+ from thermal ionization was not detectable from this material.

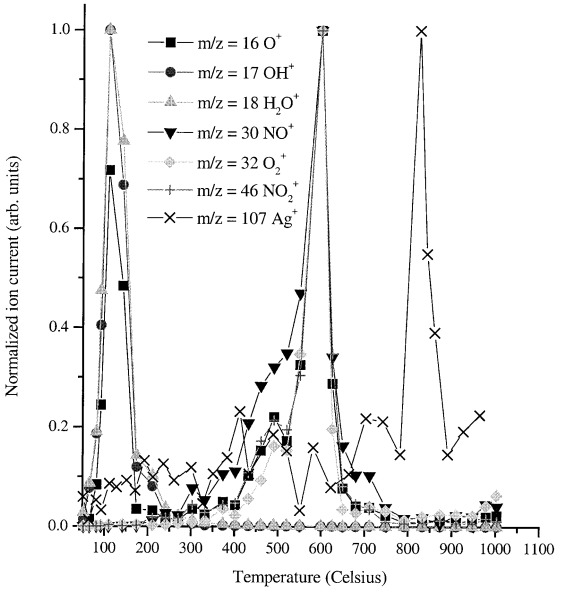

Fig. 2. Ion currents for electron impact generated ions vs. the filament temperature for the silver borosilicate with $AgNO_3$ on Ta. Each ion current is normalized to the same maximum intensity for the purpose of analyzing intensity vs. temperature behavior.

3.3.2. $AgNO_3$ on Ta

Fig. 3 shows the EI mass spectrum for $AgNO_3$ on Ta as a function of temperature. The primary difference between the results shown in Figs. 2 and 3 is the temperature at which the NO_2 was observed in the gas phase. For $AgNO_3$/Ta the NO_2 was observed at 450 °C, which is about 150 °C lower than that for the AgBS/$AgNO_3$/Ta (600 °C). There are a number of factors that could account for this difference. One possibility is that the solubility of NO_2 in the glass is great enough to retard the evaporation of NO_2. Ag^0 was initially observed over the $AgNO_3$/Ta at about 820 °C; this is similar to the behavior of the AgBS/$AgNO_3$/Ta. The similarity between these two figures suggests that the chemistry responsible for the production of neutral species of the AgBS/$AgNO_3$/Ta system is dictated, at least in part, by the thermal decomposition of the silver compound (i.e. $AgNO_3$).

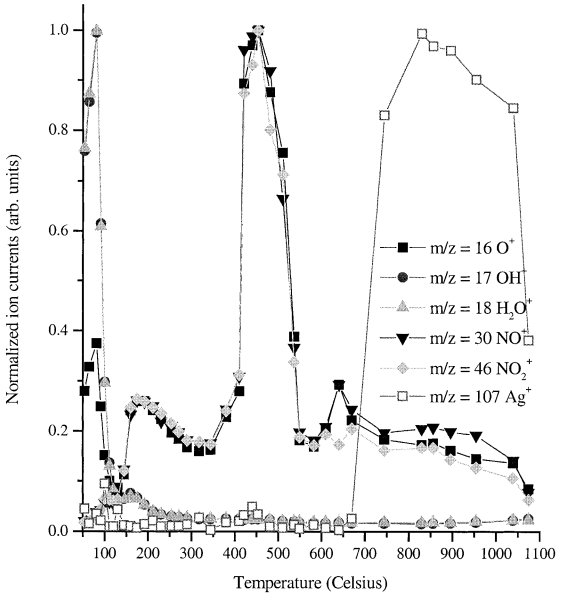

Fig. 3. Ion currents for electron impact generated ions vs. the filament temperature for $AgNO_3$ on Ta. Each ion current is normalized to the same maximum intensity for the purpose of analyzing intensity vs. temperature behavior.

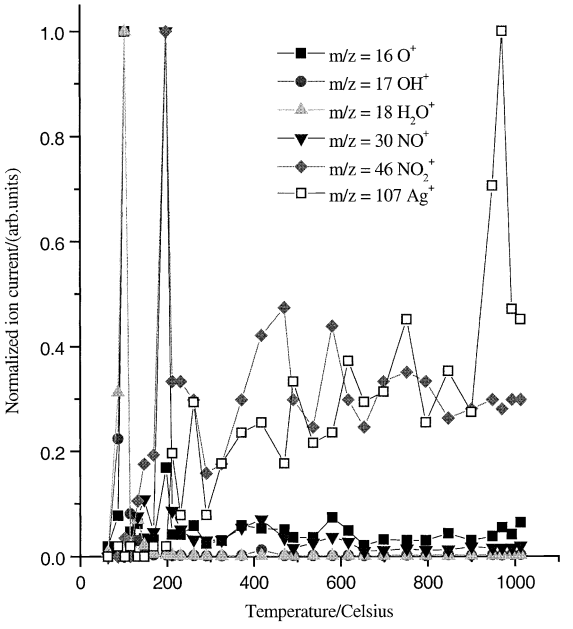

Fig. 4. Ion currents for electron impact generated ions vs. the filament temperature for the silver borosilicate with $AgNO_3$ on Re (Re containing ions are not shown). Each ion current is normalized to the same maximum intensity for the purpose of analyzing intensity vs. temperature behavior.

Ag^+ from thermal ionization was not observed during this analysis.

3.3.3. Silver–borosilicate containing Ag on Ta

The EI mass spectrum of the AgBS/Ag/Ta was essentially identical to that for $AgNO_3$/Ta and AgBS/$AgNO_3$/Ta except for the lack of signals attributable to nitrate. For the AgBS/Ag/Ta, the water appears in the gas phase at the same temperature as for the samples with $AgNO_3$ but disappears at a lower temperature. Neutral Ag sublimed from this sample across the same temperature range as was observed for the samples with $AgNO_3$. Signal due to Ag^+ from thermal ionization was not detectable from this material.

3.3.4. Silver–borosilicate containing $AgNO_3$ on Re

The EI mass spectrum of the AgBS/$AgNO_3$/Re was similar to that observed for the same borosilicate on Ta. Relative ion abundances generated by EI, versus temperature, are plotted in Fig. 4. Water and NO_2 were observed in the gas phase and are due to the sublimation of water and the decomposition of nitrate, respectively, as was the case for the AgBS/$AgNO_3$/Ta; however, the temperature at which NO_2 appeared was lower in this case than for the Ta filament experiments. This result suggests that Re is more readily oxidized than Ta. Alternately, this could also be an anomaly due to a difference in heating rates.

Another difference in the EI mass spectrum of the AgBS/$AgNO_3$/Re as compared to AgBS/$AgNO_3$/Ta was seen between 430 and 460 °C. In this temperature range, the AgBS/$AgNO_3$/Re produced Re–O species in the gas phase (which are not shown in Fig. 4 since they would increase the complexity of an already complex figure). The dominant ions, m/z = 233 and 235 ($^{185}ReO_3^+$ and $^{187}ReO_3^+$), are most likely EI-induced fragments of the parent ion $Re_2O_7^+$, which appears at m/z = 482, 484, and 486 [30,31]. It is highly unlikely that $HReO_4$ is the parent of ReO_3^+ because formation of $HReO_4$ by hydrolysis of Re_2O_7 would require the presence of water; however, the results in Fig. 4 show only one desorption peak for water and that the desorption of water ends at a

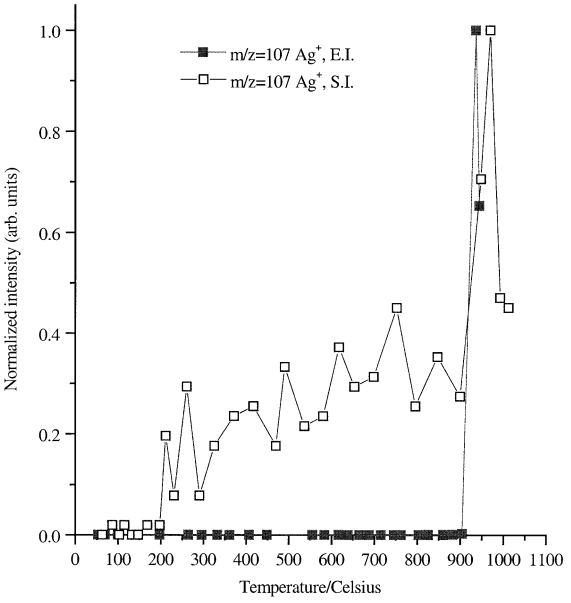

Fig. 5. Ion currents for Ag^+ produced by electron impact and surface ionization, vs. the filament temperature, for the AgBS with $AgNO_3$ on Re. Each ion current is normalized to the same maximum intensity for the purpose of analyzing intensity vs. temperature behavior. These ion currents were measured on separate samples, with different thermocouples, hence the peak maxima are well within experimental error of each other.

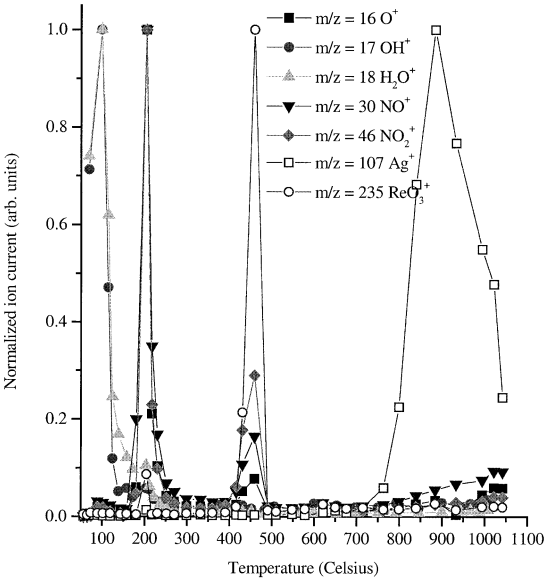

Fig. 6. Ion currents for electron impact generated ions vs. the filament temperature for the $AgNO_3$ on Re. Each ion current is normalized to the same maximum intensity for the purpose of analyzing intensity vs. temperature behavior.

temperature well below that at which the ions at $m/z = 233$, 235, 482, 484, and 486 are detected.

At about 950 °C ions resulting from Ag^0 were seen in the EI mass spectrum. This temperature is about 100 °C higher than that which was recorded for the detection of Ag^0 (by EI) during the AgBS experiments involving Ta, although it may be an artifact due to temperature measurement error.

The emission of Ag^+ from this material was significant (there was emission of thermally ionized Ag^+ from all borosilicate materials containing Ag on Re), and the temperature at which the emission of thermal Ag^+ from this sample was observed was essentially the same temperature at which the EI-generated Ag^+ was observed (see Fig. 5). The presence of Ag^+ from thermal ionization is the only significant difference in the spectra from this material on the two different filament materials. The temperature profiles of Ag^+ from EI of Ag^0 and Ag^+ from thermal ionization were essentially the same.

3.3.5. Silver–borosilicate containing Ag on Re

The only two species observed in the EI mass spectrum of the AgBS/Ag/Re system were water and Ag. Water was observed from 50 to 100 °C and Ag appeared at about 1000 °C. When nitrate was present in other samples it abetted the formation of rhenium oxides, so when nitrate was not present neither the nitrogen oxides nor the rhenium oxides were produced in measurable quantities. All samples of this material on Re produced significant beams of Ag^+, in contrast to all of the materials on Ta which did not, and the temperature profiles for Ag^0 from EI again were similar to that for Ag^+ from thermal ionization of $AgNO_3$ on Re.

3.3.6. $AgNO_3$ on Re

A plot of the EI generated ion currents versus temperature for $AgNO_3$/Re is presented in Fig. 6. The EI mass spectrum for $AgNO_3$/Re was similar to that for AgBS/$AgNO_3$/Re (Fig. 4). All the EI generated ions observed from AgBS/$AgNO_3$/Re were also observed from the $AgNO_3$/Re. The main difference between the EI mass spectra from these two samples

was the desorption temperature of the NO_2. For the $AgNO_3$ on Re, NO_2 was observed in the gas phase at about 200 °C compared to 340 °C for the AgBS/$AgNO_3$/Re. The increase in the appearance temperature of NO_2^+ from the AgBS/$AgNO_3$/Re is most likely due to an interaction of the $AgNO_3$ with the borosilicate glass, as was postulated for the AgBS/$AgNO_3$/Ta. The similarity between Figs. 4 and 6 implies that the chemistry of the AgBS/$AgNO_3$/Re is controlled by the filament material and the silver bearing compound, $AgNO_3$ and not the borosilicate glass.

All of the silver borosilicate materials on Re filaments produced beams of Ag^+, whereas none of the materials produced significant beams of Ag^+ from Ta filaments. In contrast, these materials on the two different filament materials produced roughly equal amounts of Ag^0 as observed by EI. Further, the temperature profile of Ag^+ from TIMS was the same as the temperature profile of Ag^0 from EI, indicating that the two processes are closely linked. Interestingly, Ag^0 volatilized with a very similar temperature profile for both filament materials. This suggests that the chemistry is not totally dissimilar, and that the difference in emission of Ag^+ from the materials on Re filaments is due to some factor other than the chemistry of Ag in glass. The most obvious conclusion that can be drawn from this information is that Ag is in the same state in all of these experiments, namely that it is Ag^0, and that because being dissolved in the molten glass may decrease the vapor pressure of Ag (as compared to pure Ag or $AgNO_3$ at the same temperature), it does not appreciably change the mode of vaporization. In Sec. 7 we will address the reasons for preferring the explanation that there is a significant difference in the work function of the molten glasses on different filament materials to account for the differences in ionization efficiency.

4. Computational description

4.1. Chemical systems

Two types of chemical systems were considered during the computational studies. The first represented just the molten glass on the filament, and consisted of SiO_2, B_2O_3 and the filament material of interest (Tc, Ru, Rh, Pd, Ta, W, Re, Os, Ir, and Pt). The second type of chemical system consisted of $AgNO_3$, SiO_2, B_2O_3, and either Re or Ta (to represent the filament). The amounts of the components considered were: 6.82×10^{-8} mol B_2O_3, 2.00×10^{-8} mol SiO_2, 9.27×10^{-9} mol of $AgNO_3$ (for those calculations that included $AgNO_3$), and 3.75×10^{-5} moles of filament material. We chose this chemical composition to correlate our computational work with our on-going experimental work involving these systems and with the traditional application of the silica gel method as is described in the following.

In our past studies of the Bi–B_2O_3–SiO_2 system [23], we used Si to B ratios of 1:6.82. This ratio was repeated in our present Ag–B_2O_3–SiO_2 studies, and for the sake of consistency we decided to use this mole ratio for our computational studies as well. Correlation with the traditional application of the silica gel method was more difficult because each application of the silica gel method results in a molten glass emitter of a unique chemical composition. In general, however, the total sample mass (the analyte of interest in the emission enhancing mixture) is usually in the 10–100 μg range. The amount of the analyte in the emission enhancing mixture is also quite variable. Some microanalyses require as few as 10^{10} atoms (16.6 fmol) and others as much as micromoles of the analyte of interest. Our choice of analyte metal amounts in the nanomole range falls well within the normal operational parameters for this technique. Last, our choice of the amount of filament material was based on our estimate of the approximate surface area of filament in contact with the borosilicate melt during the analysis.

4.2. Computational method and approach

Primarily, two variations of the silica gel method have been reported. In one, silica gel and H_3PO_4 were used to enhance emission; in the other, H_3BO_3 (for our calculations we used B_2O_3, the dehydrated form of H_3BO_3) is used in place of phosphoric acid. Initially, a set of preliminary calculations was performed for both the P–O and B–O systems; however,

since the thermodynamic data set for the boron oxides is more complete, only the silica gel–B_2O_3 system was addressed in detail during our present study of the emission of Ag^+ and the reactivity of the glass phase and the filament materials.

The calculations were performed using the Facility for the Analysis of Chemical Thermodynamics (FACT) Gibbs free energy minimization code EQUILIB [32], which uses the chemical composition, pressure, temperature, ensemble of possible phases, and thermodynamic quantities for those phases, to deduce the phase compositions at which the free energy is at a minimum. The algorithm used for the computation is based on the SOLGASMIX code developed by Eriksson [33]. A generalized description of code use/operation is presented in the following.

The code is menu-driven, and queries the user for input. The user provides the chemical composition, as elements or chemical "compounds" (up to 24 elements), and the temperature and pressure for which the calculation should be performed. The code provides a "list" of gaseous species, liquid phases and solid phases (from its databases) that could be considered in the calculation and the user chooses some or all of the species, phases and solutions supplied by the program. The code then attempts to compute the equilibrium phase assemblage of the system. If after 99 tries the free energy does not converge, the code gives up and returns an "estimate" of the equilibrium composition. When the code successfully completes the calculation, it returns the compositions of the gaseous, liquid and crystalline phases that are present when the free energy is at a minimum. All of the computational results discussed below are the results from calculations that converged.

In the event that the desired data are not present in the database, the user can build a user database to supplement the standard database. For the present work, it was necessary to input data for a variety of chemical species into a user database. Data sets for low-temperature liquid metal data for some of the elements of interest were also constructed. The constant pressure heat capacity (C_p) for elements and simple binary super-cooled liquids were required for modeling the behavior of the silica gel molten glass. These data sets were constructed by assigning the super-cooled liquids values of C_p equivalent to those of the pure solid at the same temperature as the super-cooled liquid of interest. Super-cooled liquid metal C_p's for Tc, Ru, Rh, Pd, Ag, Re, Os, Ir, and Pt were estimated in this way, based on the data for the crystalline phases that were present in the FACT database. In addition, C_p's for Re(g) and Re_2O_7(g) were taken from the HSC database [34]. The super-cooled liquid data are needed because some of these metals have solubilities in the molten glass at temperatures well below their normal melting temperatures.

The species and phases considered during each calculation were chosen as follows. For each calculation, every possible neutral gaseous species was selected for consideration except for the nitrate systems, for which no elemental nitrogen vapor species were selected. The choice of neutral species only was made because the temperatures under consideration were not great enough for plasma formation, while the choice of no elemental nitrogen species was made because the vapor phases for these materials (decomposing nitrates) are known to include very little elemental nitrogen species (even though N_2 is a thermodynamically favorable species under the conditions used for these calculations). The decision to include essentially all the vapor species was made for two reasons. First, it was possible that an important species might be neglected if "chemical intuition" were used for gaseous species selection. Second, there was no need to limit the size of the ensemble of species and phases considered because the sizes of the chemical systems under consideration were well below the limitations of the code.

The liquid phase was considered as a single, ideal solution. Consideration was given to using a more complex approach, such as two or more liquid phases between which the chemical species in the liquid(s) could be partitioned. This approach was rejected, however, because there was no chemical basis for introducing this complexity into the calculations. The liquid species selected for consideration included: B_2O_3, SiO_2, the filament material of choice and any stable liquid species involving that element (oxides,

borides, silicides, etc.), and Ag-containing species for those calculations involving Ag.

The crystalline phases considered included (1) the analyte metal of interest, if it was stable at the temperatures of interest, (2) any analyte metal borides, silicates and oxides that were stable at the temperatures of interest for which there were data, and (3) the filament metal, metal oxides, borides, and silicates, etc., that were stable at the temperatures of interest for which there were data. Because of the desire to address the reactivity of the glass with the other chemical species in the systems of interest, the crystalline phases SiO_2 and B_2O_3 were not usually considered. Inclusion of these phases sometimes presents a problem related to the kinetics of these systems. Since glasses are super-cooled liquids and are, by definition, thermodynamically metastable with respect to the crystalline phases that are stable at temperatures below the normal melting point of the crystalline phases, inclusion of these crystalline phases often depletes the glass of these species in a way that is not consistent with the known chemistry of these materials (molten borosilicate glasses do not generally precipitate appreciable quantities of crystalline SiO_2 and B_2O_3 at these temperatures).

5. Computational results

5.1. Chemical thermodynamics of the silver–borosilicate-tantalum system

Calculations performed to predict the chemical equilibria of systems involving Ag, borosilicate glass and Ta (as a filament material) were performed at temperatures in the range 900–1300 °C. These calculations can logically be partitioned into three sets based on the Ag source. The amounts of reactants considered were 2.00×10^{-8} mol SiO_2, 6.82×10^{-8} mol B_2O_3, 3.75×10^{-5} mol Ta, and 9.27×10^{-9} mol Ag, the latter being present in one of three forms: Ag, $AgNO_3$, or Ag_2O. The results of these calculations are shown in Table 2.

In all, four Ta-bearing crystalline phases, Ta, TaB_2, Ta_2O_5, and Ta_2Si, were predicted for the chemical systems in which silver was introduced as Ag or Ag_2O. For the system that considered silver as $AgNO_3$, a fifth crystalline phase, Ta_2N, was also predicted. What we see in these phases is that Ta reacted with every element present in the chemical system (other than Ag) to form thermodynamically stable (with regard to the glass phase) crystalline phases. At 900 °C, essentially all of the boron, nitrogen, oxygen, and silicon present in the chemical system that includes $AgNO_3$ is present in the crystalline phases (over 99.99% of the boron, even a greater percentage of the nitrogen, 99.99% of the oxygen, and 99.82% of the silicon), with the remainder present in the vapor phase. As the temperature increases, this changes somewhat because the vapor pressures of the boron- and silicon-bearing vapor species increase, while at the same time Ta_2Si becomes thermodynamically less stable until it disappears somewhere between 1100 and 1200 ° C. These results clearly show that the thermodynamic stabilities of the crystalline Ta-bearing phases are so great that, under equilibrium conditions, they would be expected to destroy the glass phase.

To summarize, there were numerous similarities with these three sets of calculations. First is the prediction that there would not be a stable glass phase under any of the conditions considered. Second, essentially all of the B and Si is found in the crystalline phases TaB_2 and Ta_2Si at all but the highest temperature (Ta_2Si decomposes between 1200 and 1300 °C). Third, the partial pressure of Ag was predicted to be independent of temperature and the form in which Ag was introduced, indicating that all the Ag was present in the vapor phase. Last, the pressures of Ta(g), TaO(g), and TaO_2(g) were invariant to changes in Ag-bearing starting material (and the oxygen content of the chemical system), at constant temperatures of (900 and 1000 °C), suggesting these species are in chemical equilibrium with one another and with Ta_2O_5, which is predicted to be present at all three temperatures.

5.2. Chemical thermodynamics of the silver–borosilicate–rhenium system

Calculations performed to predict the chemical equilibria of systems involving Ag and borosilicate

Table 2
Computational results for silver–borosilicate glass systems with Ta filament[a]

Form of Ag considered	$T = 900\ ^{\circ}C$			$T = 1000\ ^{\circ}C$			$T = 1300\ ^{\circ}C$		
	Ag	Ag_2O	$AgNO_3$	Ag	Ag_2O	$AgNO_3$	Ag	Ag_2O	$AgNO_3$
Vapor pressures (atm)									
Ag	9.27×10^{-9}	9.27×10^{-9}	9.27×10^{-9}	9.27×10^{-9}	9.27×10^{-9}	9.27×10^{-9}	9.27×10^{-9}	9.27×10^{-9}	9.27×10^{-9}
Ta	3.62×10^{-28}	3.62×10^{-28}	3.62×10^{-28}	1.94×10^{-25}	1.94×10^{-25}	1.94×10^{-25}	4.30×10^{-21}	2.47×10^{-19}	2.47×10^{-19}
TaO	3.62×10^{-18}	3.62×10^{-18}	3.62×10^{-18}	4.13×10^{-16}	4.13×10^{-16}	4.13×10^{-16}	7.56×10^{-13}	1.56×10^{-11}	1.56×10^{-11}
TaO_2	1.36×10^{-17}	1.36×10^{-17}	1.36×10^{-17}	1.69×10^{-15}	1.69×10^{-15}	1.69×10^{-15}	3.49×10^{-13}	7.51×10^{-11}	7.51×10^{-11}
O	3.05×10^{-22}	3.05×10^{-22}	3.05×10^{-22}	6.04×10^{-20}	6.04×10^{-20}	6.04×10^{-20}	2.72×10^{-16}	8.15×10^{-15}	8.15×10^{-15}
O_2	4.83×10^{-28}	4.83×10^{-28}	4.83×10^{-28}	3.20×10^{-25}	3.20×10^{-25}	3.20×10^{-25}	9.63×10^{-21}	6.17×10^{-19}	6.17×10^{-19}
BO	6.11×10^{-14}	6.11×10^{-14}	6.11×10^{-14}	3.50×10^{-12}	3.50×10^{-12}	3.50×10^{-12}	2.14×10^{-9}	2.82×10^{-8}	2.82×10^{-8}
SiO	3.57×10^{-11}	3.57×10^{-11}	3.57×10^{-11}	1.07×10^{-9}	1.07×10^{-9}	1.07×10^{-9}	2.00×10^{-8}	2.00×10^{-8}	2.00×10^{-8}
NO			9.89×10^{-25}			4.34×10^{-22}			3.23×10^{-16}
Crystalline phases (mole)									
Ta	3.73×10^{-5}	3.73×10^{-5}	3.73×10^{-5}	3.73×10^{-5}	3.73×10^{-5}	3.73×10^{-5}	3.74×10^{-5}	3.74×10^{-5}	3.73×10^{-5}
TaB_2	6.82×10^{-8}	6.82×10^{-8}	6.82×10^{-8}	6.82×10^{-8}	6.82×10^{-8}	6.82×10^{-8}	4.86×10^{-8}	4.86×10^{-8}	4.86×10^{-8}
Ta_2O_5	4.89×10^{-8}	4.98×10^{-8}	5.45×10^{-8}	4.87×10^{-8}	4.96×10^{-8}	5.43×10^{-8}	3.71×10^{-8}	3.80×10^{-8}	4.26×10^{-8}
Ta_2Si	2.00×10^{-8}	2.00×10^{-8}	2.00×10^{-8}	1.89×10^{-8}	1.89×10^{-8}	1.89×10^{-8}	0	0	0
Ta_2N			9.27×10^{-9}			9.27×10^{-9}			9.27×10^{-9}

[a] The vapor species and crystalline phases predicted during the calculations are listed in the first column, with the quantities of vapor species being partial pressures (in atmospheres) and the quantities of crystalline phases being numbers of moles (there were no stable liquid phases predicted for the calculations with Ta as the filament material). The three temperatures at which the calculations were performed are listed in the second row, with the initial state of the Ag in the calculation (as Ag metal, Ag_2O, or $AgNO_3$) listed in the third row. Beneath the second row (temperature) and third row headings (the form of Ag) are the partial pressures and number of moles associated with each of the species/phases listed in the first column. No nitrogen-bearing species are listed for those calculations that did not include Ag as $AgNO_3$ (as there was no nitrogen present in the chemical system).

Table 3
Computational results for silver–borosilicate glass systems with Re filament[a]

Form of Ag considered	$T = 900\ °C$			$T = 1000\ °C$			$T = 1300\ °C$		
	Ag	Ag_2O	$AgNO_3$	Ag	Ag_2O	$AgNO_3$	Ag	Ag_2O	$AgNO_3$
Vapor pressures (atm)									
Ag	8.76×10^{-9}	8.76×10^{-9}	8.76×10^{-9}	9.21×10^{-9}	9.21×10^{-9}	9.21×10^{-9}	9.27×10^{-9}	9.27×10^{-9}	9.27×10^{-9}
Re	2.86×10^{-27}	2.86×10^{-27}	2.86×10^{-27}	1.33×10^{-24}	1.33×10^{-24}	1.33×10^{-24}	1.18×10^{-18}	1.18×10^{-18}	1.18×10^{-18}
Re_2O_7	1.34×10^{-29}	6.61×10^{-10}	2.65×10^{-9}	2.07×10^{-26}	6.42×10^{-10}	2.62×10^{-9}	4.69×10^{-19}	1.31×10^{-18}	3.82×10^{-17}
O	2.93×10^{-17}	1.91×10^{-14}	2.32×10^{-14}	2.25×10^{-15}	5.11×10^{-13}	6.25×10^{-13}	4.04×10^{-11}	4.68×10^{-11}	7.58×10^{-11}
O_2	4.44×10^{-18}	1.88×10^{-12}	2.80×10^{-12}	4.44×10^{-16}	2.28×10^{-11}	3.41×10^{-11}	1.52×10^{-11}	2.03×10^{-11}	5.33×10^{-11}
BO_2	2.69×10^{-13}	6.87×10^{-12}	7.59×10^{-12}	1.23×10^{-11}	1.85×10^{-10}	2.04×10^{-10}	5.41×10^{-8}	5.78×10^{-8}	7.09×10^{-8}
SiO	9.40×10^{-15}	1.44×10^{-17}	1.18×10^{-17}	5.20×10^{-13}	2.30×10^{-15}	1.88×10^{-15}	6.35×10^{-9}	5.62×10^{-9}	3.82×10^{-9}
NO			9.25×10^{-9}			9.27×10^{-9}			9.27×10^{-9}
Glass mole fraction									
B_2O_3	0.729	0.729	0.729	0.730	0.730	0.730	0.560	0.551	0.512
SiO_2	0.214	0.214	0.214	0.214	0.214	0.214	0.376	0.385	0.424
Re	0.052	0.052	0.052	0.055	0.055	0.055	0.064	0.064	0.064
Ag	0.005	0.005	0.005	<0.001	<0.001	<0.001	<0.000 01	<0.000 01	<0.000 01
Crystalline phases (mole)									
Re	3.75×10^{-5}	3.75×10^{-5}	3.75×10^{-5}	3.75×10^{-5}	3.75×10^{-5}	3.75×10^{-5}	3.75×10^{-5}	3.75×10^{-5}	3.75×10^{-5}

[a] The vapor species and crystalline phases predicted during the calculations are listed in the first column, with the quantities of vapor species being partial pressures (in atmospheres), the quantities of the species present in the liquid phase being the mole fraction, and the quantities of crystalline phases being numbers of moles. The three temperatures at which the calculations were performed are listed in the second row, with the initial state of the Ag in the calculation (as Ag metal, Ag_2O, or $AgNO_3$) listed in the third row. Beneath the second row (temperature) and the third row headings (the form of Ag) are the partial pressures and number of moles associated with each of the species/phases listed in the first column. No nitrogen-bearing species are listed for those calculations that did not include Ag as $AgNO_3$ (as there was no nitrogen present in the chemical system).

glass, with Re as a filament material, were performed at temperatures in the range 900–1300 ° C. These calculations can logically be partitioned into three sets based on the Ag source. For each set the amounts of reactants considered were 2.00×10^{-8} mol SiO_2, 6.82×10^{-8} mol B_2O_3, 3.75×10^{-5} mol Re, and 9.27×10^{-9} mol Ag, the latter being present in one of three forms: Ag, $AgNO_3$ or Ag_2O. The results of these calculations are shown in Table 3. There were numerous similarities with these three sets of calculations. First, the predicted pressure of Ag and the mole fraction of Ag in the glass phase for each were independent of the origin of the Ag at all temperatures. The results predict that the solubility of Ag in the melt decreases with increasing temperature. Accompanying this decrease in solubility is an increase in the Ag pressure with temperature over this same temperature interval. Ag is quite volatile at all temperatures above its melting point, and it is expected that it will be rapidly depleted from the molten glass at the higher temperatures. These results are in agreement with the known high temperature behavior of the phases Ag_2O and $AgNO_3$, which decompose at temperatures well below 900 °C to form Ag(s) and gaseous species [35]. Second, at no temperature was the presence of Ag(s) predicted, even though Ag melts at 961 °C, which is well above 900 °C, the lowest temperature at which calculations were performed. This is no doubt due to the predicted stability of the glass phase, which dissolves the Ag to form a solution that is thermodynamically more stable than the ensemble of Ag(s) and borosilicate glass.

Further evidence supporting solution stability is the predicted chemical behavior of Re. The solubility of Re in the glass phase also shows temperature dependence, increasing with increasing temperature. This behavior is expected in that these temperatures are far below the melting temperature of Re. The Re solubility in the glass melt shows no dependence, however, on the chemistry of Ag, Ag_2O or $AgNO_3$; it is predicted to be the same at each temperature regardless of the source of the Ag. The distribution of the remaining Re between the vapor and crystalline phases is, however, dependent on the oxidation potential of the chemical systems under consideration because of the high volatility of crystalline Re–O phases. At temperatures as low as 1027 °C, the most refractory Re–O phase, ReO_2, has a considerable Re_2O_7 (the only Re–O vapor species expected to be present in appreciable amounts over condensed Re–O phases) vapor pressure of about 5.0×10^{-3} atm. This means that all crystalline Re–O phases are predicted by the thermodynamics to be very volatile. An unknown factor is the kinetics of the conversion of the ReO_2 phase to Re_2O_7. This conversion may be slow enough to allow sufficient ReO_2 buildup on the surface of the molten glass to affect the surface properties. The computational results are in agreement with the known chemistry of Re. At 900 °C, the predicted pressure of Re_2O_7(g) is about 10^{19} greater when Ag is introduced as Ag_2O than when it is introduced as Ag. This is consistent with the experimental results that showed the presence of Re oxides in the gas phase for the Ag nitrate samples, whereas the samples with Ag did not. This can be explained by the nitrate oxidizing Re metal.

The form of the Ag-bearing phase also affects the glass-forming constituents. When Ag is introduced with oxygen, as Ag_2O or $AgNO_3$, the excess oxygen and/or NO_x species generated by the thermal reduction of Ag to the elemental state react with the B_2O_3 in the glass, forming BO_2(g). This effect can be seen at 900 °C, where the calculations involving Ag_2O and $AgNO_3$ predict a BO_2(g) pressure about 25 times greater than that predicted by the calculations with Ag.

A large unknown in all of these calculations is the fact that there is no thermodynamic data available for the formation of the perrhenate anion, ReO_4^-. This ion has been observed from some molten glass materials [23] but is not accounted for in these calculations because thermodynamic data for this species in the glass are not available. This species might play an important role in the formation of a Re–O species on the surface that could account for the formation of a high work function surface as is postulated in a later section. Since perrhenate is ionic and the other species are not, it is conceivable that perrhenate has a much lower vapor pressure, and hence may build up to significant concentrations, sufficient to have an effect

on the work function of the surface. For example, it is known that $Ba(ReO_4)_2$ is relatively stable in this temperature range as is demonstrated by the fact that ReO_4^- emitters that have operated in this temperature range for up to 2 years have been developed [27,28].

5.3. Chemical thermodynamics of borosilicate–filament material systems

The metals considered for this computational study were Tc, Ru, Rh, Pd, Ta, W, Re, Os, Ir, and Pt. The molar amounts of the three components considered, SiO_2, B_2O_3, and the filament metal of interest were the same as for the calculations with Ag, 2.00×10^{-8} mol SiO_2, 6.82×10^{-8} mol B_2O_3, and 3.75×10^{-5} mol of filament metal. Calculation were performed in the range 900–1300 °C. The predicted behaviors of these materials fell into three groups. The first group included only Pd, which is predicted to be exceeding soluble in the glass. The second group included Rh and Ta. These metals were predicted to destroy the glass phase. The third group included Tc, Ru, W, Re, Os, Ir, and Pt. These metals exhibited chemical behaviors that appear to be compatible with their use as a filament material for the silica gel method. The most significant factor affecting the outcome of the calculations was the ability of the filament metal to reduce the borosilicate glass.

Of the metals considered, Pd was unique. Its melting point, 1552 °C, is more than 200 °C less than the next lowest melting point metal considered, Pt (1769 °C). As was observed in the earlier calculations involving Ag, the solubility of Pd in the melt tends to increase, with increasing temperature, at temperatures below its melting point. This behavior is also exhibited in the predicted behavior of Pd. At 900 °C, its mole fraction in the melt was 0.837; at 1300 °C, its mole fraction was 0.861. At such high mole fractions of Pd, this solution would no longer be a molten glass solution, with small amounts of dissolved metal. Instead it would more likely behave like a metal, with enough solute added to it to decrease its melting point. This "reaction" between the molten glass and the filament would be likely to result in significant erosion of the filament.

The second group of prospective filament materials included Rh and Ta. The modeling results predict that these two metals are likely to destroy the molten glass by reacting with it, although the reaction products for the two are quite different. For Rh, the computational results at 900, 1000, 1100, and 1200 °C predicted that there would be a stable molten glass, with mole fractions of the Rh in the melt increasing from 0.134 at 900 °C to 0.150 at 1200 °C. At 1300 °C, it was predicted that the molten glass would no longer be stable. The chemical reaction that appears to destroy the molten glass is a reaction to form $RhO_2(g)$ that preferentially consumes B_2O_3 in the glass phase.

The situation for Ta is even more severe. The computational results predict that Ta will destroy the molten glass at all temperatures in the range 900–1300 °C. At all temperatures, crystalline Ta, TaB_2, Ta_2O_5, and Ta_2Si were predicted to be present. At 900 °C, 99.99% of the oxygen was predicted to be present as Ta_2O_5; at 1300 °C, the percentage was 75.76%, with the remainder present in oxygen-bearing vapor species. It is likely that the kinetics will be slow enough that these reactions will not go to thermodynamic equilibrium, but they could be a cause of the poor ionization efficiency from Ta filaments.

The third group of prospective filament materials included Tc, Ru, W, Re, Os, Ir, and Pt. The modeling results suggest that these metals should perform well as filament materials. These modeling results predict that the high temperature equilibria of molten glass systems that include these metals should exhibit low metal (filament metal) vapor pressures as compared to molten glass systems with Pd and Rh. In addition, all of these metals except Pt (mole fraction in the glass of 0.295 at 1100 °C) have low solubilities (mole fractions of 0.108 or less at 1100 °C). These low solubilities are not surprising since these metals are quite refractory, with Pt being the lowest melting of the group (melting temperature of 1769 °C).

The results predict that there should be no stable crystalline filament metal–oxygen phases present in the molten glass at temperatures in the range 900–1300 °C. The oxides of these elements are all volatile, and other than WO_3 (which melts at about 1837 °C)

all of them have low melting or decomposition temperatures (in the range 40–477 °C). If stable crystalline oxide phases of the filament metals were present, then the molten glass phase would probably be destroyed. We were not able to predict the solubilities of these oxides in the glass phase because the thermodynamics of these oxide phases are largely unknown at temperatures above their normal stability ranges. When compared to the behavior of other prospective filament materials, the pressures of the metal oxide vapor species are predicted to be roughly equivalent to, or lower than, those of the molten glass systems including Pd, Rh, and Ta. The vapor pressures of the oxide species from the molten glasses containing Tc, Ru, W, Re, Os, Ir, and Pt, when contrasted with the pressures of PdO over the chemical system containing Pd, are expected to be lower because Pd and its oxide are considerably more volatile. As compared to the behavior of the Rh and Ta containing molten glass systems, however, these results might initially appear to be surprising because Re–O, W–O, and Tc–O phases are generally thought of as being quite volatile as compared to Ta–O phases. This apparent discrepancy is due to the fact that the amount of oxygen available to Rh and Ta to form metal oxide species is considerably greater than that available to Re, W, or Tc. Rh and Ta are strong enough chemical reductants to destroy the borosilicate glass and reduce species such as B_2O_3 and SiO_2, whereas Tc, Re, and W are not strong enough reducers to effect the same chemical reactions.

The low solubilities of these metals in the glass phase is not surprising since these metals are quite refractory, with Pt being the lowest melting of the group. The modeling results predict that Pt would be the most soluble (in the molten glass) of these metals, with mole fractions of 0.245 and 0.338 at 900 and 1300 °C, respectively. Rhenium and W were the least soluble in the molten glass. At 900 °C, the mole fractions of Re and W in the molten glass were 0.052 and 0.039, respectively; at 1300 °C, their mole fractions were 0.064 and 0.133, respectively. The solubilities of Tc, Ru, Os, and Ir were greater than that of Re at 900 °C, and less than that of W at 1300 °C.

6. Discussion

6.1. Decomposition of $AgNO_3$

There were some results from the experiments involving $AgNO_3$ that were unexpected and difficult to explain. Specifically, the NO_2^+ ion intensity showed two maxima, although this character was less pronounced in the case of $AgNO_3$ on Re (without borosilicate glass). In an attempt to understand this behavior, we looked at thermal decomposition results from other workers who had reported using Ta containers (or did not report the container material) for their studies of the thermal decomposition of nitrate salts [31,36–39]. The thermal decomposition of nitrate salts, $AgNO_3$ among them, has been extensively studied at least in part because it appears that there is not one “mechanism” that can adequately describe the decomposition of these materials. From the thermochemical modeling studies we performed, we found that the reaction of $AgNO_3$ with Ta is spontaneous at temperatures as low as room temperature, which suggests that as the temperature increases it is possible that there could have been interactions between the crucible material (Ta) and $AgNO_3$ during the previously published TGA and mass spectrometric studies performed to deduce the decomposition mechanism.

Although we were not able to find any precedence for the variations in the NO_2^+ intensities observed and have no explanation for the observed phenomena, we believe that our results show clearly that the decomposition of the nitrate anion plays a role in the chemistry of the molten silica gel systems. For the experiments that employed a Re filament, abundant Re–O vapor species were not observed unless Ag had been introduced as the nitrate. During the Ta filament experiments, there was no mass spectrometric evidence of reaction of the filament with the nitrate because of the low vapor pressures of the Ta–O phases at these low temperatures; however, in our earlier studies of the bismuth–borosilicate system there were marked differences in the behavior of the samples supported on Ta and Re filaments [23].

An obvious conclusion from these studies is that

the decomposition of $AgNO_3$ can be influenced by the container material. The reactivity of $AgNO_3$ at the decomposition temperature is such that most, if not all, metallic container materials will react with the $AgNO_3$. This helps to explain the diversity of results of $AgNO_3$ decomposition in the literature. It is conceivable that the decomposition temperature of $AgNO_3$ is a function of the container material. If a truly inert metallic container does not exist, and our data suggests that this may be the case, then the decomposition temperature can only be described in association with a specific container material. This is particularly true when dealing with thin coatings of $AgNO_3$ on a filament. It is likely that a refractory oxide container would be more inert than a metallic one, since the molten glass is an oxide itself.

6.2. Formation and emission of thermal ions from molten borosilicate solutions

Based on the experimental results and the chemical thermodynamics of the Ag, Ag–O, and Ag–N–O borosilicate systems, it appears that the hypothesis that the silica gel method is dependent solely on the emission of pre-formed ions present in the molten borosilicate glass is implausible. Both Ag_2O(s) and $AgNO_3$(s) decompose at quite low temperatures, producing Ag metal and vapor species. In addition, both the experimental results and the computational results support the concept that Ag^0 is stable both in the molten borosilicate matrix at elevated temperatures and when the pure materials are heated. Experimentally, Ag^+ emission from these borosilicate glasses occurred over a temperature range indistinguishable from the temperature range over which the Ag^0 volatilized (within our ability to measure sample temperatures). At these temperatures, only the zero oxidation state for Ag seems likely. These facts lead to a hypothesis quite different from the pre-formed ion hypothesis. Instead, these data support the concept that Ag is first dissolved in the molten glass as individual atoms. The Ag then evaporates from the molten glass solution as a mixture of neutrals and ions, with the majority of the ions being formed at the glass–vapor interface and not within the glass or at the glass–filament interface. Lastly, we believe the work function of the molten glass surface plays a significant role in ion formation and emission. In support of this hypothesis we present the following evidence.

During the present studies involving silver–borosilicate, Ag ions were detected in both the EI and TIMS operational modes. Because the voltages for the ion optics of the ion–neutral instrument for both operating modes discriminate against ions produced by the other mode, these results unequivocally support the hypothesis that both neutrals and ions are emitted from the molten borosilicate glass. Further, there is a significant overlap between the temperature profiles for the emission of Ag^0 and Ag^+, demonstrating that the two species are volatilizing at essentially the same temperature. However, while the volatilization rate of Ag^0 is approximately equal for all of the materials tested on both Re and Ta filaments, the emission of Ag^+ by TIMS was orders of magnitude greater from the materials on Re filaments. This demonstrates that there is something unique about the glass melted on the Re filament that greatly enhances ion formation. In addition, the temperature profiles of both Ag^0 and Ag^+ from all materials was the same within experimental error (with respect to the temperatures at which the species appeared), giving a strong indication that these two species might be volatilizing by the same process, but that some are being ionized while some are neutrals. The question is, “what determines the ratio of ions to neutrals?”

Results from past work in our laboratory [23] showed that Bi^+ and ReO_4^- ions are emitted directly from the surface of the borosilicate glass, not from the filament nor the filament glass interface and that this is the predominant mode of ion emission from the molten glass emitters. We hypothesize that the work function of the surface is modified by the presence of the dissolved Re, which is oxidized either in the melt or at the glass-vapor interface, forming ReO_2, ReO_3, ReO_4^-, or some other Re–O species, thus increasing the work function of the surface of the glass and enhancing the formation of thermal ions. Although the neutral Re–O species are quite volatile at operating temperature, it has been previously demonstrated that various perrhenate salts, such as the barium salt,

have only modest volatility at these temperatures. Thus, this hypothesis is based, at least in part, on the belief that the glass surface alone probably does not have a work function great enough to result in the observed ion emission. The work functions of SiO_2 and B_2O_3 are both near 5 eV [40] at the temperatures attained during the silica gel process, whereas the work function of Re oxides is reported to be as high as 7.2 eV for a heated, oxidized Re surface (in the range 1000–1200 K) under an oxygen partial pressure range of $1–5 \times 10^{-5}$ Torr [41]. Even at temperatures as high as 1500 K the work function was still greater than 6.5 eV. Such a high work function would result in the formation of considerably more ions than a clean Re metal surface with a work function of about 5.0 eV.

The Saha-Langmuir equation:

$$\frac{n_+}{n_0} = \frac{g_+}{g_0} \frac{(1 - r_+)}{(1 - r_0)} \exp \frac{(\phi - \mathrm{IP})}{RT} \quad (1)$$

where ϕ is the work function of a surface at which ionization is occurring, IP is the ionization potential of the ions formed, g_+ and g_0 are the respective statistical weights for the ion and its related neutral vapor species, r_+ and r_0 are the respective reflection coefficients for the ion and neutral species, R is the gas constant, T is the absolute temperature, and n_+/n_0 is the emission ratio of positive ions and neutral species from the surface, was developed assuming conditions somewhat different than those present on these molten glass surfaces; however, there are some similarities. For example, both in the assumptions upon which the Saha-Langmuir equation is based, and for the molten glass ion emitters, the vapor species volatilize as a mixture of atoms and neutrals. We believe that in both cases the ratio of ions to neutrals will be influenced by the ionization potential of the volatilizing atoms (since this is a measure of the energy required to strip an electron from a volatilizing atom) and by the work function of the surface (since this is a measure of the ability of a surface to strip an electron from a volatilizing atom).

An additional piece of evidence suggesting that the Saha-Langmuir theory might be applicable are the results of Scheer and Fine, which demonstrate that the self-surface ionization of positive and negative ions from W and Re filaments is described quite well by the Saha-Langmuir theory [42]. Self-surface ionization is similar to the proposed ion formation mechanism since it involves volatilization of atoms from a surface as a mix of neutrals and ions. In the ensuing discussion we will attempt to test the applicability of this theory to the processes associated with the emission of ions and neutrals from molten glass surfaces.

For species volatilizing from the surface, the reflection coefficients are zero, since these are for gases reflecting from the surface without making thermal contact. Then we can estimate the Ag^+/Ag^0 ratio emitted from the molten glass surface if it had a work function equivalent to that of an oxidized Re surface. Assuming that $g_+/g_0 = 1$, $r_+ = r_0 = 0$, $\phi = 7.20$ eV, IP = 7.57 eV and $T = 1000$ K, the Saha-Langmuir theory predicts that the ratio of singly charged ions to neutrals emitted from the surface to be 0.0136. This prediction of an ion formation efficiency of greater than 1% is sufficient to explain the success of the silica gel method as an ion formation medium. Values of ϕ measured for a clean Re surface or of a SiO_2 or B_2O_3 surface have typically been about 5 eV. When this value for ϕ is used in the equation, the ratio is about 1.11×10^{-13}. The reason for this large shift in the ratio of ions to neutrals is a consequence of the fact that the difference between IP and ϕ is in the exponential term of Eq. (1). In addition, the solubility of Re in the melt suggests that some Re–O species may be present at the glass–vapor interface, which is the same surface from which the thermal ions are emitted.

7. Conclusions

Based on past work performed in our laboratory [23], and on the experimental and modeling results presented in this article, we can draw some conclusions about how the choice of filament material impacts the ion emission process. In our past work, which involved the bismuth–borosilicate system with Ta and Re as filament materials, the ion intensity

measurements for $Bi^+(g)$ were up to 100 times lower for melts supported on the Ta filament as compared to those on Re. Our present computational results predict that Ta reacts extensively with the borosilicate glass. We hypothesize that this reactivity is manifested in two ways. First, Ta can react with both SiO_2 and B_2O_3; the thermodynamically favored reaction is the one with B_2O_3. As the crystalline Ta reacts with B_2O_3 in the glass, it changes the glass composition. Instead of a B_2O_3/SiO_2 of approximately 3.5, as was the initial ratio in both our past and our present experimental studies, the ratio would be expected to be much lower. Such a change in the composition of the glass could have a dramatic effect, possibly impacting the solubility of analyte metal (Bi or Ag) in the glass and/or altering the mechanism by which ions are formed. In addition, depletion of B_2O_3 would result in a higher-melting, more viscous, glass which could reduce the diffusion rates of the analyte species (Bi or Ag) to the glass–vapor interface from which they evaporate. Second, as Ta_2O_5, Ta_2Si, and TaB_2 are formed, their impact on the behavior of the glass is unknown, but not likely to be beneficial. Although our equilibrium modeling suggests that the Ta filament would completely destroy the glass solution, consuming both the B_2O_3 and SiO_2, it is likely that these chemical systems are slow to attain equilibrium. Such a situation is in agreement with our past results [23], in which we detected Ta in the residues of bismuth–borosilicate melts, none of which were completely destroyed by reaction with the Ta metal. It is not possible to predict how a change in glass composition would impact ion formation, but the experimental evidence suggests that degrading the glass greatly decreases ion formation efficiency, even though the neutral Ag species appears to volatilize in roughly the same fashion from all of the materials tested.

It is hypothesized that the molten borosilicate glass has four important roles to play in this process. First, it acts as a solvent for the analytes, Re and the oxides of Re. Second, it provides the oxygen necessary to oxidize Re, particularly when excess oxygen in the form of nitrate is present. The thermodynamic calculations cannot predict whether Re is oxidized before or after it is dissolved in the molten glass, and we suspect that it may proceed along both paths. Third, the dissolved Re–O species provide a high work function surface that greatly enhances ion formation efficiency. Fourth, the metallic Re may help to reduce some elements to the zero oxidation state, although in the case of Ag that apparently is not a factor since the Ag compounds probably reduce spontaneously at modest temperatures even in the molten oxide matrix. The metallic atoms in the molten glass then volatilize with a certain percentage being stripped of an electron by the attraction of the surface for an electron as measured by the work function. When the value of the work function approaches the ionization potential of the volatilizing atom, the ionization efficiency is favorable, whereas it is highly unfavorable when the difference approaches 2 eV. The Saha-Langmuir theory may or may not be a reasonable absolute representation of this process, but in any event the general features of the theory are consistent with the experimental results, in particular the ionization efficiency increasing exponentially as the work function of the surface approaches the ionization potential of the analyte.

One piece of information that would complement this study is the measurement of the work function of these molten glass surfaces. The results of such measurements could be used to confirm the hypothesis that the Re oxide species in the molten glass enhances the work function that in turn enhances ion formation efficiency. Unfortunately, we do not have access to an apparatus to perform these measurements.

These studies were limited to the ion formation process of Ag^+ from molten glass ion emitters, and the question then arises as to applicability of the proposed mechanism to the many other elements that are analyzed by various silica gel methods. It is possible that elements such as Bi, Cd, and Pb are also reduced to the zero oxidation state in molten glasses and produce ions by the same or a similar mechanism as with Ag. However, there are several elements that are analyzed by variations of these methods that are not readily reduced to the zero oxidation state. These elements may share some of these characteristics,

such as some chemical species of the element being dissolved in the molten glass, and the surface having an enhanced work function due to the presence of Re oxides on the surface. For example, it is improbable that the alkaline earth elements are reduced to the zero oxidation state, and these elements are analyzed by variations of the silica gel technique. Ion formation methods of this type require independent study.

The picture that emerges from these studies is that there is a delicate balance between the oxidative/reductive properties of the molten glass and the reactivity of the filament material. The glass cannot react too readily with the filament material or the glass phase will be destroyed; yet it has to be sufficiently reactive to allow the Re–O species to be formed on the surface to increase the work function to the point where there is efficient ion formation. However, the fact that Ag^+ was efficiently formed in the molten glass in which there were few or no Re–O species detected in the EI mode suggests that only a minimal amount of the Re–O phase needs to be produced to promote efficient ion formation.

Last, we believe our mass spectral and thermochemical modeling results indicate that some of the theories associated with the decomposition of nitrate salts (especially $AgNO_3$) presently held might need to be revisited, especially those based on experiments that employed Ta containers for the nitrate salts. In fact, it may be that the decomposition of $AgNO_3$ can only be studied as a function of the container material, and that past studies need to be categorized as to the container used in the decomposition testing. Our past experimental results [23] indicated that, at high temperatures, the choice of support material for molten glasses has an impact on the evolution of vapor species, and our thermochemical modeling results show that Ta, in the presence of oxygen-bearing species at high temperatures, can be oxidized by metal nitrates at temperatures as low as a few hundred degrees Celsius, which could result in the accelerated decomposition of these materials as compared to the decomposition rates when the materials are in contact with a more nearly inert container material (such as alumina).

Acknowledgements

This work was performed at the Idaho National Engineering and Environmental Laboratory. The authors wish to thank the reviewers, whose comments helped strengthen the manuscript, and to acknowledge the financial support of the United States Department of Energy, Basic Energy Sciences program, under contract no. 3ED102.

References

[1] A.E. Cameron, D.H. Smith, R.L. Walker, Anal. Chem. 41 (1969) 525.
[2] K. Azmy, J. Veiser, B. Wenzel, M.G. Massett, P. Copper, Geol. Soc. Am. Bull. 111 (1999) 475.
[3] I.L. Barnes, T.J. Murphy, J.W. Gramlich, W.R. Shields, Anal. Chem. 45 (1973) 1881.
[4] J.H. Beattie, A. Macdonald, J.J. Harthill, J.R. Bacon, J. Nutr. Biochem. 2 (1991) 512.
[5] A. Broekman, J.G. van Raaphorst, Fres. Z. Anal. Chem. 318 (1984) 398.
[6] J.R. De Laeter, M.T. McCulloch, K.J.R. Rosman, Earth Planet. Sci. Lett. 22 (1974) 226.
[7] J.R. De Laeter, N. Mermelengas, Geostand. Newslett. 2 (1978) 9.
[8] T.M. Esat, D.E. Brownlee, D.A. Papanastassiou, G.J. Wasserburg, Science 206 (1979) 190.
[9] W.R. Kelly, F. Tera, G.J. Wasserburg, Anal. Chem. 50 (1978) 1279.
[10] W.R. Kelly, P J. Paulsen, Talanta 31 (1984) 1063.
[11] R.D. Loss, K.J.R. Rosman, J.R. De Laeter, Talanta 30 (1983) 831.
[12] N. Mermelengas, J.R. De Laeter, K.J.R. Rosman, Geochim. Cosmochim. Acta 43 (1979) 747.
[13] P.J. Paulsen, W.R. Kelly, Anal. Chem. 56 (1984) 708.
[14] K.J.R. Rosman, J R. De Laeter, Int. J. Mass Spectrom. Ion Phys. 16 (1975) 385.
[15] K.J.R. Rosman, J.R. De Laeter, A. Chegwidden, Talanta 29 (1982) 279.
[16] C.L. Smith, J.R. De Laeter, K.J.R. Rosman, Geochim. Cosmochim. Acta 41 (1977) 676.
[17] F. Tera, G.J. Wasserburg, Anal. Chem. 47 (1975) 2214.
[18] E. Waidmann, K. Hilpert, J.D. Schladot, M. Stoeppler, Fres. Z. Anal. Chem. 317 (1984) 273.
[19] E. Waidmann, K. Hilpert, M. Stoeppler, Fres. J. Anal. Chem. 338 (1990) 572.
[20] C.S.J. Briche, P.D.P. Taylor, P. De Bièvre, Anal. Chem. 69 (1997) 791.
[21] A. Götz, K.G. Heumann, Int. J. Mass Spectrom. Ion Processes 83 (1988) 319.
[22] K.R.D. Rosman, R.D. Loss, J.R. De Laeter, Int. J. Mass Spectrom. Ion Processes 56 (1984) 281.

[23] T. Huett, J.C. Ingram, J.E. Delmore, Int. J. Mass Spectrom. Ion Processes 146/147 (1995) 5.
[24] J.E. Delmore, T. Huett, J.E. Olson, A.D. Appelhans, Int. J. Mass Spectrom. Ion Processes 155 (1996) 149.
[25] J.E. Delmore, A.D. Appelhans, J.E. Olson, Int. J. Mass Spectrom. Ion Processes 140 (1994) 111.
[26] D.A. Dahl, SIMION 3D, Version 6.0, User's Manual, INEL-95/0403, Idaho National Engineering Laboratory, Idaho Falls, ID, 1995.
[27] J.E. Delmore, A.D. Appelhans, E.S. Peterson, Int. J. Mass Spectrom. Ion Processes 108 (1991) 179.
[28] J.E. Delmore, A.D. Appelhans, E.S. Peterson, Int. J. Mass Spectrom. Ion Processes 146/147 (1995) 15.
[29] A.D. Appelhans, D.A. Dahl, J.D. Delmore, Anal. Chem. 62 (1990) 1679.
[30] P. Ausloos, C. Clifton, O.V. Fateev, A.A. Levitsky, S.G. Lias, W.G. Mallard, A. Shamin, S.E. Stein, O.D. Sparkman, J.A. Sparkman, NIST Standard Reference Database 1A, NIST Mass Spectral Search Program and The NIST/EPA/NIH Mass Spectral Library. Version 1., U.S. Department of Commerce, National Institute of Standards and Technology, Gaithersburg, MD, 1995.
[31] M. Afzal, M. Saleem, H. Ahmad, Sci. Int. (Lahore) 2 (1990) 285.
[32] C.W. Bale, A.D. Pelton, W.T. Thompson, Facility for the Analysis of Chemical Thermodynamics (F*A*C*T) 2.1 - User Manual, Ecole Polytechnique de Montreal/Royal Military College, Canada, 1996.
[33] G. Eriksson, Chem. Scr. 8 (1975) 100.
[34] A. Roine, HSC Chemistry® for Windows 3.0, Outokumpu Research Oy, Pori, Finland, 1997.
[35] N.N. Greenwood, A. Earnshaw, Chemistry of the Elements, 1st ed., Pergamon, Elmsford, NY, 1984, pp. 1373 and 541.
[36] D.J. Anderton, F.R. Sale, Proceedings of the First European Symposium on Thermal Analysis, D. Dollimore (Ed.), University of Salford, UK, Heyden, London, 1976, p. 278.
[37] J.G. Jackson, A. Novichikhin, R.W. Fonseca, J.A. Holcombe, Spectrochim. Acta, Part B 50 (1995) 1423.
[38] J.G. Jackson, R.W. Fonseca, J.A. Holcombe, Spectrochim. Acta Part B 50 (1995) 1449.
[39] B.V. L'vov, A.V. Novichikhin, Spectrochim. Acta Part B 50 (1995) 1427.
[40] V.S. Fomenko, Handbook of Thermionic Properties. Electronic Work Functions and Richardson Constants of Elements and Compounds, Plenum, New York, 1966, p. 69.
[41] W.D. Davis, Environ. Sci. Technol. 11 (1977) 587.
[42] M.D. Scheer, F. Fine, J. Chem. Phys. 46 (1967) 3998.